**Natural Hazards
and Earth System
Sciences**

Open Access

Discussions

Lightning characteristics in Eastern Mediterranean thunderstorms during different synoptic systems

Y. Ben Ami[1], O. Altaratz[1], Y. Yair[2,3], and I. Koren[1]

[1]Department of Earth and Planetary Sciences, Weizmann Institute of Science, Rehovot, Israel
[2]School of Sustainability, Interdisciplinary Center (IDC), Herzliya, Israel
[3]Department of Life and Natural Sciences, The Open University of Israel, Ra'anana, Israel

Correspondence to: I. Koren (ilan.koren@weizmann.ac.il)

Discussion Paper | Discussion Paper | Discussion Paper | Discussion Paper |

NHESSD

3, 3655–3685, 2015

Lightning characteristics in Eastern Mediterranean thunderstorms

Y. Ben Ami et al.

Title Page

Abstract | Introduction

Conclusions | References

Tables | Figures

◄◄ | ►►

◄ | ►

Back | Close

Full Screen / Esc

Printer-friendly Version

Interactive Discussion

Abstract

Thunderstorms activity takes place in the Eastern Mediterranean mainly along the boreal fall and winter seasons during synoptic systems of Red Sea Trough (RST), Red Sea Trough that closed a low over the sea (RST-CL), and Cyprus Low (during fall – FCL and Winter – WCL). In this work we used the Israeli Lightning Location System ground strokes dataset (between October 2004 and December 2010) for studying the lightning strokes properties and their link to the thermodynamic conditions in each synoptic system.

It is shown that the lightning activity dominates over sea during WCL and FCL systems (with maximum values of 37 strokes per $25\,km^2\,day^{-1}$ in WCL, and 54 in FCL) and have a dominant component over land during the RST and RST-CL days. The stronger instability (high CAPE values of $621 \pm 466\,J\,kg^{-1}$) during RST-CL days together with the higher altitude of the clouds' mixed-phase region ($3630 \pm 316\,m$) result in higher ground strokes density during this system (compared to all other) but lower fraction of positive ground strokes ($3 \pm 0.5\,\%$). In general the fraction of positive strokes was found to be positively correlated with the wind shear values in the layer between 0 and $-25\,°C$. It increases from the $1.2 \pm 1\,\%$ in early fall to $17 \pm 7\,\%$ in late winter, (during FCL and WCL days) and can be linked to the decrease in the sea surface (and lower troposphere) temperature during those months, due to an impact on the charge centers vertical location.

The diurnal cycle in the lightning activity was examined for each synoptic system. During WCL conditions no preferred times were found along the day (as it relates to the timing of frontal systems). During the fall systems (FCL and RST-CL) there is a peak in lightning activity during the morning hours, probably related to the enhanced convection driven by the convergence between the eastern land breeze and the western synoptic winds. The distributions of peak currents in FCL and WCL systems also change from fall to winter and include more strong negative and positive strokes toward the end of the winter.

1 Introduction

Thunderstorms in the Eastern-Mediterranean (EM) region are associated with three synoptic systems: Cyprus Low (CL), Red Sea Trough (RST), and with a hybrid system of Red Sea Trough that closes a low over the sea (RST-CL), (Levin et al., 1996; Altaratz et al., 2003; Ziv et al., 2009). Those storms occur between the boreal fall and early spring (September–April). Throughout summer the area is influenced by the subsidence of the subtropical high that inhibits deep convection.

CL is a mid-latitude low pressure system that is usually generated in the bay of Genoa near the lee side of the Alps (Buzzi and Tibaldi, 1978) and moves eastwards over the Mediterranean-Sea (Alpert et al., 1990; Shay-el and Alpert, 1991). The low level low is accompanied by an upper level trough that transports cold air into the region. According to Shalev et al. (2011) who analyzed lightning activity over the region, more than 71 % of winter-time lightning flashes and 41 % of fall ones occur under this synoptic system. While transported over the Mediterranean, the cold continental air mass is destabilized and its moisture content increases due to the interaction with the warm sea. In proximity to the eastern coast of the Mediterranean Sea, the friction due to the land–sea interface and the convergence between the western synoptic winds and the eastern land-breeze, further aids convection (Heiblum et al., 2011; Ziv and Yair, 1994; Ziv et al., 2009). Under such conditions thunderclouds develop over the sea, and then are advected into land.

RST is a low-level trough that extends from the African Monsoon along the Red-Sea towards the EM (Dayan et al., 2001; Kahana et al., 2002). When the upper level trough location enables southern winds in the mid-troposphere, it triggers transport of tropical moisture towards the EM. Under such conditions thunderclouds generally develop over the south and eastern part of the EM, exhibiting relatively high cloud-bases, ~ 2–3 km above sea-level. These conditions occur mainly along fall months (October–November), and are associated with ~ 43 % of the flashes at this time of the year (Shalev et al., 2011). In some cases the RST system extends towards the

Mediterranean-Sea and forms a close low over the sea, in a complex hybrid situation. Here we named this type of system as RST-CL.

Previous works that studied lightning activity over Israel used two types of measuring systems. Levin et al. (1996) investigated the link between the polarity of lightning strokes and the ambient wind conditions using the Tel-Aviv CGR3 lightning flash counter. Yair et al. (1998) used the same detection system for examination of the ratio between intra-cloud (IC) to cloud-to-ground flashes along the year. Both works were limited to a small domain around the city of Tel-Aviv due to the short detection range of the CGR3 instrument (Mackarres and Darveniza, 1994). Altaratz et al. (2003) and Shalev et al. (2011) surveyed the climatology of ground lightning flashes over a period of several years using data from the national Israel Lightning Location System (ILLS). Altaratz et al. (2003) investigated lightning characteristics over land vs. over the sea while Shalev et al. (2011) discussed the link between the temporal-spatial properties of lightning strokes and the synoptic conditions. They proposed that spatial patterns of lightning strokes can be used as a proxy for the prevailing synoptic condition.

In the present work we study the thermodynamic conditions during specified synoptic systems and their link to the generation of lightning strokes and their properties. We focus on the main synoptic systems that produce electrical activity over the EM: (a) WCL, (b) FCL, (c) RST and (d) RST-CL. So the ground strokes characteristics, during these four synoptic systems, are analyzed and linked to the prevailing thermodynamic conditions.

2 Data and methods

2.1 Israel Lightning Location System (ILLS)

The ILLS is composed of eight sensors located along Israel (marked on Fig. 5). The present configuration consists of three types of sensors: five are electric field based, two are magnetic field sensors and one is a combined sensor that monitors both mag-

netic and electric fields. The detection algorithm is based on the time of arrival and magnetic field direction techniques to retrieve information on the peak current intensity, polarity, location and time of impact of ground strokes. The data used in this study was retrieved by the ILLS between October 2004 and December 2010. During the period
5   between 2004 and 2007 only seven detectors were operational.

The detection efficiency over Israel, where the point of impact is covered by all sensors, is estimated to be 80–90 % (Yair et al., 2014). The spatial detection accuracy over this region is $\sim$ 500 m and the temporal resolution for detection of successive strokes is $\sim$ 15 μs. The detection efficiency decreases as moving away from the network cen-
10   ter (Katz and Kalman, 2009). At distances that are larger than 100 km from the Israeli coastline it is estimated to be only 50 %.

In this study we analyzed strokes data and not flashes. Based on Shalev et al. (2011) findings the multiplicity of cloud-to-ground flashes detected by the ILLS is 1.1 (using thresholds of 1 km and 0.2 s). Therefore we choose to use the raw strokes data as
15   it represents flash data to a good approximation and it does not force the usage of thresholds.

2.1.1   Sensitivity test of detection efficiency

As stated above, the detection efficiency of the ILLS depends on the distance from the center of the network. To reduce errors caused by undetected weak strokes we
20   investigate the detection efficiency as a function of location and peak current. The focus is on negative strokes because weak positive strokes, with peak currents smaller or equal to 10 kA, are excluded from the dataset since they are considered as attributed partly to intra-cloud discharges (Cummins et al., 1998).

The detection efficiency is estimated here by analyzing the distributions of peak cur-
25   rents as a function of distance from the center of the ILLS detectors network. The center was determined here at 32°4 N and 35° E and the analysis was done for days of WCL only. However, similar results are obtained for the other synoptic systems as well.

Full Screen / Esc

Printer-friendly Version

Interactive Discussion

CC BY

The distributions for specified narrow peak currents ranges are presented as a function of longitudes (Fig. 1a and c) and latitudes (Fig. 1b and d). Black boxes mark a distance of 250 km from the approximate center of the ILLS (marked by a black arrow).

Figure 1 shows that small peak current strokes (< 10 kA) are detected only near the center of the detectors' array. This difference is more pronounced in the longitudinal direction. In order to avoid this bias to small currents near the center of Israel, we chose to eliminate negative strokes with peak currents smaller than 10 kA from the analysis.

In order to obtain sufficient statistics, from one hand, and to minimize errors due to detection efficiency, on the other hand, the study region is limited to a radius of 250 km from the ILLS center. In addition, days with less than 20 detected strokes are excluded from the dataset. Detailed description of the ILLS detection efficiency and location errors is given by Kats and Kalman (2009) and Manoochehrnia et al. (2007).

2.2 Classification of lightning strokes according to the synoptic system

Daily parameters of lightning strokes i.e., peak current intensity [kA] and polarity, location [lat. and long. degree] and time of impact in ground [UTC], are grouped according to the prevailing synoptic conditions and the season. The seasons are defined according to the boreal seasonal distribution: September to November as fall and December to February as winter. The synoptic conditions (see Table 1) are defined based on examination of daily maps in $1° × 1°$ resolution of wind direction at 925 hPa and mean sea level pressure, produced by the Global Data Assimilation System (GDAS, Kanamitsu, 1989). The maps of 12:00 and 24:00 UTC are examined with respect to the timing of the detected strokes.

For specifying CL conditions, the following criteria are used: (a) a center of low pressure at sea level, located north or west of the Israeli coast, (b) northwest to southwest winds at 925 hPa level over the central coast of Israel and (c) the absence of significant low pressure system south of Israel. *For condition of RST* the criteria are (a) a center of low pressure at sea level located south or south-east of Israel, (b) northeast to

Full Screen / Esc

Printer-friendly Version

Interactive Discussion

southeast winds at 925 hPa and (c) the absence of dominant low system north or west of the Israeli coast. *For conditions of RST-CL*: (a) two distinct centers of low pressure, one located south of Israel and the other one north (or west) of the Israeli coast and (b) western winds in low levels. Only days that precisely meet the above criteria (see Table 1) are selected for the analysis. Hence the presented analysis does not cover the entire occurrence of lightning in the study region (17.3 % of the strokes data is omitted from the analysis).

The classification of lightning days for the four synoptic systems produced 51, 15 and 12 lightning days for the conditions of CL, RST-CL and RST, respectively, for the fall season. The corresponding numbers of strokes is 80 861, 57 026 and 5118. For the conditions of WCL, 128 lightning days with a total of 98 963 strokes are analyzed.

The GDAS dataset was also used for determination of thermodynamic conditions during each synoptic system. The height of the 0 and $-25\,^\circ$C isotherms and the Convective Available Potential Energy (CAPE) values were estimated for the area between 32°–33° N and 34°–35° E as representative values for our study area.

2.3 MODerate resolution Imaging Spectro-radiometer (MODIS)

Data from the MODIS instrument onboard the Aqua satellite is used for estimation of sea surface temperature (SST). The temperature is estimated for the marine area bounded between 30°–34° N and 32°–36° E, using the 11 µm band and in spatial resolution of 16 km^2.

3 Results

This section presents characteristics of lightning strokes over the EM analyzed for specified synoptic condition and season. It includes three subsets for the fall season RST, RST-CL and FCL, and one subset for the winter season, WCL. The link to the thermodynamic conditions is examined first.

3.1 Thermodynamic conditions

First the characteristic thermodynamic conditions prevailing during each synoptic system are examined because they determine the properties of thunderclouds (e.g.: vertical dimension, updraft speed, water and ice content) and hence the electrical activity.

Figure 2 presents the height and depth (thickness) of the atmospheric layer located between the 0 and $-25\,^{\circ}\text{C}$ isotherm levels. In this atmospheric layer resides the mixed phase region of clouds that is the most relevant to the non-inductive charging mechanism which involves graupel and ice particles and supercooled water (Takahashi, 1978; Saunders et al., 1991; Saunders, 2008). Examination of the vertical location and depth of this atmospheric layer as a function of synoptic condition and season can shed light on the potential for thunderstorms development and lightning production.

During the WCL days the $0\,^{\circ}\text{C}$ isotherm is located around $2 \pm 0.5\,\text{km}$ (Fig. 2, y axis), much lower than its mean location in the fall synoptic systems, due to the much colder conditions prevailing in the winter. During RST conditions, the location of the $0\,^{\circ}\text{C}$ isotherm is the highest ($3.7 \pm 0.5\,\text{km}$), and it is $3.4 \pm 0.4\,\text{km}$ during RST-CL, and $3.1 \pm 0.5\,\text{km}$ during FCL. It means that the mixed phase region in thunderclouds during the fall season is located higher in the atmosphere, compared to the winter thunderclouds, with the RST thunderclouds located in the highest position within this season (Fig. 2, red centroid).

The depth of this atmospheric layer, between 0 and $-25\,^{\circ}\text{C}$ (Fig. 2, x axis) can teach us about the instability of the atmosphere during thunderstorms events. It can be deduced from the thermal lapse rate along this atmospheric layer, where we expect to find the mixed-phase region in thunderclouds. A thinner layer implies more unstable conditions, meaning a larger lapse rate (a difference of $25\,^{\circ}\text{C}$ along a shorter distance). Deeper layer, on the other hand, represents smaller instability. During RST conditions this atmospheric layer is the thinnest, hence represents the most unstable conditions compared to the other three synoptic systems.

The instability of the atmosphere can be represented by the mean CAPE as well. The CAPE represents the entire atmospheric column and not only the specific layer between 0 and −25 °C as examined in Fig. 2, and it is a commonly used parameter for characterization of the thermodynamic conditions during thunderstorms. Figure 3

5   presents the daily CAPE values per synoptic system as a function of the daily number of detected strokes. Centroids of the four synoptic systems are marked in circles. The relative position of the mean CAPE values for the four different synoptic systems is quite similar to the one showed in Fig. 2 by the depth of the layer between the 0 and −25 °C. Clearly, a general increase trend in ground strokes production, with the

10   increase in CAPE values, is observed. The trend is in agreement with many previous studies conducted around the globe (Randell et al., 1994; Williams and Stanfill, 2002) and in Israel (Shalev et al., 2011). Larger CAPE values (stronger instability) that characterize the synoptic systems of the fall season can better support the required conditions for charge separation within thunderclouds. Those requirements for efficient charging

15   include strong updrafts (Deierling and Petersen, 2008), and enhanced graupel and ice mass fluxes (Deierling et al., 2008). These factors have been shown to be correlated with stronger electrical activity. So the conditions during the RST-CL events create the strongest instability and as a consequence, the best conditions for electrification (as expressed by the daily number of strokes in Fig. 3). During the fall season the tem-

20   perature of the lower atmosphere and the SST (see Sect. 3.2.4.b) are still fairly high therefore the combination with cold air in the upper troposphere creates very unstable conditions (Ziv et al., 2009).

The RST data in Fig. 3 (red circle) is exceptional regarding the fall season systems and is located below the line connecting the other synoptic systems data. It represents

25   fewer strokes for high values of CAPE, which seems to contradict the previous findings. A possible explanation for this contradiction is higher relative fraction of IC flashes that are not detected by the ILLS. The IC flashes can be attributed to the relatively higher-altitude of the mixed phase region in the clouds during the RST days, as implied by the higher level of the 0 °C isotherm in Fig. 2. Clouds located higher in the atmosphere

are expected to produce higher ratio of IC to CG flashes (Pierce, 1970; Prentice and Mackerras, 1977; Yair et al., 1998).

It can be noticed that the characteristic CAPE values during fall and winter thunderstorms in Israel are small compared to CAPE values measured around the globe during summer thunderstorms ($\sim$ 1000's $J\,kg^{-1}$, Williams and Renno, 1993; Williams et al., 2005). The CAPE in our region is similar to other winter thunderstorms like the ones typical for Japan (Suzuki et al., 2011).

A positive linear correlation between the CAPE values and the number of strokes per day is found for WCL ($R = 0.41$) and FCL ($R = 0.46$). The two linear fits and equations are presented in Fig. 3. The rate of increase in the number of strokes per day, on the order of 4.6 strokes per unit of CAPE, is similar in both seasons.

Next we examine in more details the characteristics of the lightning strokes and their link to the thermodynamic conditions.

3.2 Characteristics of lightning strokes

3.2.1 Number of daily strokes as a function of month and synoptic system

Figure 4 shows the monthly averages of number of strokes per day (bars) for the four synoptic systems subsets. The average number of thunderstorm days per month is plotted in red curve. The error-bars indicate the inter-annual variation per month.

The highest electrical activity per thunderstorm-day occurs during October in RST-CL system ($2734 \pm 974\,day^{-1}$). The smallest number of strokes per day is for the FCL system during September. This may be attributed to the very small dataset for this month that includes only one day with 85 strokes. The inter-annual variability in the number of strokes per day (indicated by black error-bars) is very large for the fall months. It demonstrates the large inter annual variability in the magnitude of electrical activity. There are on average only a few days of electrical activity during these months. During winter, on the other hand, the inter-annual variance is small with a mean value of 733 ± 97 (Fig. 4d).

The level of electrical activity per day, as measured by the number of ground strokes, is highly correlated with the mean value of CAPE per specific synoptic system (Fig. 3). The high flash number per day, during RST-CL systems is supported by the relatively high CAPE values during these thunderstorms days and is in agreement with Ziv et al. (2009).

3.2.2 Spatial distribution

The general spatial distribution of lightning strokes detected by the ILLS exhibits a butterfly shape, as is clearly shown in Fig. 5c. This phenomenon is a direct result of the system configuration and the resultant detection efficiency, due to the elongated position of the sensors. The western part of the detection area that spreads mostly over the sea and coastal regions is electrically active during all synoptic systems (Fig. 5a–d). The eastern region that covers a continental area, mainly over eastern Israel, Jordan and Syria, is mostly associated with lightning activity during RST and RST-CL systems.

Under conditions of WCL, the higher strokes density is detected over the sea and near the coast (Fig. 5a). This location of stronger electrical activity can be associated with larger instability over the sea during the winter, as the sea is a source for moisture and heat (Shay-El and Alpert, 1991). In addition, the convergence of the eastern land-breeze with the prevailing western synoptic wind near the coast is a key mechanism for enhanced convection and intensification of thunderclouds (Heiblum et al., 2011). During FCL days, the strokes density over the sea is larger than in WCL days and the region of high density is wider. This can be explained by the higher instability during FCL days (higher CAPE, Fig. 3) which enables significant convection over the whole eastern Mediterranean Sea, without the help of convergence near the shore like in the winter. For the RST and RST-CL days there is high activity both over the sea and over land. During RST conditions the main region of activity is determined by the location of the trough's axis. A western axis, with regard to the coast line, creates a significant activity over the sea and an eastern axis over land. This is the reason for the two separate centers that are shown in Fig. 5d.

These results demonstrate again the higher strokes' density during fall compared to the winter season. The average values of number of strokes per pixel ($25\,km^2$) per day are much higher in Fig. 5b and c compared to Fig. 5a. Maximum daily values of strokes per $25\,km^2$ are 37 in WCL, 54 in FCL, 33 in RST and 131 in RST-CL.

3.2.3 Diurnal cycle

The diurnal cycle of lightning activity during different synoptic systems is presented in Fig. 6. It shows significant differences in the timing of activity between the various systems. For example, the lightning occurrence during RST and FCL synoptic conditions, both during fall, exhibits opposite cycles. In RST conditions the cycle has of two peaks of higher electrical activity, one centered in the afternoon hours (around 17:00 LT), and a second peak in the middle of the night (around 24:00 LT, Fig. 6a). The afternoon peak demonstrates the significance of solar land heating that drives stronger convection.

During FCL, on the other hand, there is one single peak in electrical activity centered at morning times, around 09:00 LT (Fig. 6c). The likelihood for lightning activity during late morning hours is ∼ 50 % higher than in the evening hours. This diurnal cycle can be explained by the build-up of the convergence near the coast during the night and early morning, between the synoptic western wind and the eastern land breeze that reaches its maximal magnitude in the early morning hours. During RST-CL system (Fig. 6b) the single peak near 06:00 LT is less significant and is earlier than the morning peak in the FCL system. During the rest of the time the likelihood is almost constant at ∼ 3 %. During winter, under WCL conditions, the probability is ∼ 4 % along the entire day, suggesting that the likelihood of electrical activity at any given hour is about equal (Fig. 6d). This could be related to the timing of the passage of cold fronts over the study region. Yet, one can see two minor peaks centered around 06:00 and 22:00 LT. The early morning peak is similar to the one found for the conditions of RST-CL and similar to what was reported by Altaratz et al. (2003) for CL conditions.

3.2.4 Fraction of positive strokes

The relative part of positive strokes, out of total cloud to ground strokes, as a function of month and for different synoptic systems is presented in Fig. 7. Rakov and Uman (2003) discussed a global upper average limit of 10 %. Our results show that under FCL and WCL systems there is a strong increase in the fraction of positive strokes along the months. The fraction increases from 1.2 ± 1 % in early fall (FCL) to 17 ± 7 % at late winter (WCL). Higher fraction of positive strokes during winter storms was observed in previous studies over this region (Yair et al., 1998) and studies conducted worldwide (e.g.: Hojo,1989; Ezcurra et al., 2002; Finke and Hauf, 1996).

This tendency in the fraction of positive strokes emphasizes the impact of the changing thermodynamic conditions on thunderclouds properties and hence on the processes of charge separation. Rakov and Uman (2003) reviewed several mechanisms that can explain an increase in the fraction of positives stokes in the cold season. The first mechanism is related to the decrease in the distance between the positive charge center in the cloud and the ground. During winter, due to the decrease in the tropospheric temperatures and in the altitude of the mixed phase region in clouds (see Fig. 2), the upper positive charge center is closer to the ground. This may increase the probability of positive strokes. Additional proposed mechanism is the better exposure of the upper positive charge center, located near cloud top and in the anvil, to the ground due to stronger wind shear in the winter (Brook et al., 1982; Levin et al., 1996; Williams and Yair, 2006).

To further explore the dependence of positive strokes' fraction on local thermodynamic factors, we examine its link to the (a) wind-shear and (b) SST in the next section.

a. Wind shear

Yair et al. (1998) and Levin et al. (1996) showed an exponential dependence of the relative part of positive ground flashes on the wind shear over Israel. Following the above studies and using the GDAS database we estimate wind-shear according to the prevailing winds at the levels of 0 and $-25\,°C$ isotherms (not shown).

Our results propose a linear dependence under conditions of CL, with regression coefficients of 0.29 for FCL and 0.32 for WCL. The correlations suggest that for an increase in wind shear of $1\,s^{-1}$ the fraction of positive strokes increases by ~ 15 to 18 %. This finding supports the hypothesis of the "tilted dipole" (Brook et al., 1982): when the cloud is tilted the screening of the upper positive charge center from the negatively charged surface is less effective and thus the likelihood for positive strokes from the upper positive charge center increases.

The different fraction of positive strokes during WCL and FCL systems conditions, even with similar magnitudes of wind-shear, suggests that the generation of positive strokes is strongly related to the thermodynamic conditions of the atmosphere (Fig. 3) and the vertical dimension of the clouds (Fig. 2), which was shown to be different under these two synoptic systems.

b. SST

The contribution of SST, as a key factor controlling the thermodynamic conditions of the troposphere is examined here. Figure 8 shows a strong monthly negative correlation ($R = -0.99$) between the SST and the fraction of positive strokes. The dependence shows that for every $\sim 1.5\,°C$ decrease in SST there is a linear increase of ~ 1 % in the fraction of positive strokes. The colder the sea surface, the larger is the fraction of positive ground strokes.

This finding supports the suggested mechanism of higher fraction of positive strokes due to smaller distance between the upper positive charge center in the cloud and the surface, as discussed above. According to this idea the likelihood for positive strokes increases with decreasing SST due to the derived impact on the temperature of the atmosphere, the smaller vertical development of the cloud and the distance of the positive charge center from the ground (Kitagawa and Michimoto, 1994). Figure 2 indeed indicates that the mixed-phase layer base height is lower by ~ 1–$1.5\,km$ during the winter season.

3.2.5   Distributions of peak currents

Figure 9a presents the peak currents distributions for negative and positive strokes for the four synoptic systems. There are more negative strokes than positive ones under all synoptic systems (Fig. 9a). The median peak current for the negative strokes in all systems is similar, between −18.1 and −20 kA. The positive strokes distribution has a longer tail meaning higher probability for larger peak currents compared to the negative strokes. Therefore their distributions' median values, for the different synoptic system are at least 20 % higher than the corresponding absolute negative values.

The larger subsets for FCL and WCL conditions enable us to follow variations in the monthly peak currents distributions, from early fall to late winter for condition of CL. Figure 9b presents the monthly peak currents distributions for negative and positive strokes, between September and February. Over time, both the fraction and maximal magnitude of strong currents of both polarities increase. Similar trends have been observed over the east coast of the United States (Orville et al., 1987) and over the Sea of Japan (Hojo et al., 1989). The zoom-in window (Fig. 9c) demonstrates that the increase in strong currents comes simultaneously with a decrease in the fraction of weak negative currents between −35 and −10 kA. The reasons for the increase in magnitude of the strong currents along the year are unclear, and will be studied in future work.

4   Discussion and conclusions

The main synoptic systems that produce thunderstorms over the eastern Mediterranean are Red Sea Trough (RST), Red Sea Trough that closed a low over the sea (RST-CL) and Fall Cyprus Low (FCL) during fall, and Cyprus Low during the winter (WCL). This study presents the statistical properties of lightning strokes over the Eastern Mediterranean (spatial and temporal distribution, diurnal cycle, fraction of positive strokes and distribution of peak currents) as a function of season and synoptic condi-

tion, i.e.: synoptic systems. These lightning properties are directly related to the thermodynamic conditions prevailing during each system (Ziv et al., 2009).

During RST conditions the thunderclouds are located higher in the atmosphere (the level of the 0 °C isotherm is 3.7 ± 0.5 km) and the atmosphere is very unstable (mean CAPE value of 515 ± 615 J kg^{-1}). The source of moisture for these clouds is in mid-troposphere transport from Africa (Kahana et al., 2002). The mean number of ground strokes per day is $\sim 80\%$ lower compared to RST-CL days, even though the difference in the CAPE values is minor between those two types of synoptic systems. A possible reason for this difference can be the higher location of the thunderclouds in RST events that can suggest higher production of IC flashes that are not detected by the ILLS. This assumption is in agreement with Yair et al. (1998) who reported a maximum in the IC to CG ratio in the fall. Under RST conditions the strokes are distributed mostly over the sea or over land, east and south of Israel but less over the central and northern parts. The main peak of activity is in late afternoon and in the middle of the night. However, there is some uncertainty with these results due to the small dataset measured for this synoptic system. The low fraction of positive strokes ($2.5 \pm 0.8\%$) is correlated with the higher location of the mixed-phase part of the thunderclouds in the atmosphere, that leads to a larger distance between the upper positive charge center in the thundercloud and the ground (Rakov and Uman, 2003).

During RST-CL events the mean CAPE values are about 17 % higher (621 ± 466) compared to during RST events and the average daily amount of ground strokes is about five times larger. The strokes are distributed over the sea and above the entire land area of Israel. There is a peak in the thunderstorms electrical activity during early morning hours, correlated with the time of maximal convergence over the sea between the synoptic west wind and the easterly land breeze (Heiblum et al., 2011). Although the wind shear is comparable to what is found for WCL conditions, the average fraction of positive strokes in RST-CL is only $3 \pm 0.5\%$, similar to the RST case. This can be explained by the large vertical separation between cloud base and the surface, which inhibits discharge from the upper positive charge center.

Another type of synoptic system that appears in the fall months is the FCL. This synoptic system is similar to the WCL system as evident from the position of the low pressure in the surface maps. The difference between the two seasons is in the thermodynamic conditions driving significant differences in the properties of thunderclouds and their lightning strokes production.

During FCL the $0\,°C$ isotherm is located about one km higher in the atmosphere compared to its location in WCL days. The CAPE is about three times higher in FCL events and the mean number of strokes per day is about two times larger. The geographic center of the electrical activity is over the sea during both systems. The diurnal cycle of FCL presents a peak in late morning times while during WCL there is no significant peak, likely due to the arbitrary temporal passage of the cold fronts which is the major driver of the electrical activity.

The trend in the fraction of positive strokes steadily increases from $1.2 \pm 1\,\%$ in FCL days in September (early fall) to $17 \pm 7\,\%$ in WCL systems in February (late winter). We note that during CL events (combining both FCL and WCL) the fraction of the positive strokes is correlated with the wind shear (within the 0 and $-25\,°C$ layer) and inversely correlated with the SST. A colder environment suggests shorter distance between the positive charge centers and the ground. This finding is in agreement with other studies that pointed to higher fraction of positive strokes in winter storms in Japan (Suzuki, 1992).

The distributions of peak currents in CL conditions also change from fall to winter and include more strong negative and positive strokes toward the end of the winter, with larger median peak currents of positive strokes. This finding is in agreement with observation of lightning properties in winter storms in Japan, where similar conditions occur (Matsui and Hara, 2014).

Overall, the electrical activity over the eastern Mediterranean is somewhat unique with respect to mid-latitude and equatorial regions, as it takes place during fall and winter and not during summer time. It resembles the electrical activity in the Japanese

winter in many respects (Williams and Yair, 2006). The winter conditions dictate smaller vertical extent and weaker dynamics.

Further work is needed to better quantify the link between the statistical properties of lightning strokes and the macro/micro physical properties of thunderclouds. Such research has the potential to better quantify the complex relationships between the dynamic and thermodynamic conditions that together determine the nature of electrical activity by thunderstorms.

References

Alpert, P., Neeman, B. U., and Shay-El, Y.: Climatological analysis of Mediterranean cyclones using ECMWF data, Tellus A, 42, 65–77, doi:10.1034/j.1600-0870.1990.00007.x, 1990.

Altaratz, O., Levin, Z., Yair, Y., and Ziv, B.: Lightning activity over land and sea on the eastern coast of the Mediterranean, Mon. Weather Rev., 131, 2060–2070, doi:10.1175/1520-0493(2003)131<2060:LAOLAS>2.0.CO;2, 2003.

Brook, M., Nakano, M., Krehbiel, P., and Takeuti, T.: The electrical structures of the Hokuriku winter thunderstorms, J. Geophys. Res., 87, 1207–1215, doi:10.1029/JC087iC02p01207, 1982.

Buzzi, A. and Tibaldi, S.: Cyclogenesis in the lee of the Alps: a case study, Q. J. Roy. Meteor. Soc., 104, 271–287, doi:10.1002/qj.49710444004, 1978.

Cummins, K. L., Murphy, M. J., Bardo, E. A., Hiscox, W. L., Pyle, R. B., and Pifer, A. E.: A combined TOA/MDF technology upgrade of the US National Lighting Detection Network, J. Geophys. Res., 103, 9035–9044, doi:10.1029/98JD00153, 1998.

Dayan, U., Ziv, B., Margalit, A., Morin, E., and Sharon, D.: A severe autumn storm over the middle-east: synoptic and mesoscale convection analysis, Theor. Appl. Climatol., 69, 103–122, doi:10.1007/s007040170038, 2001.

Deierling, W. and Petersen, W. A.: Total lightning activity as an indicator of updraft characteristics, J. Geophys. Res., 113, 598, doi:10.1029/2007JD009598, 2008.

Deierling, W., Petersen, W. A., Latham, J., Ellis, S., and Christian, H. J.: The relationship between lightning activity and ice fluxes in thunderstorms, J. Geophys. Res., 113, D15210, doi:10.1029/2007JD009700, 2008.

Ezcurra, A., Areitio, J., and Herrero, I.: Relationships between cloud-to-ground lightning and surface rainfall during 1992–1996 in the Spanish Basque Country area, Atmos. Res., 61, 239–250, doi:10.1016/S0169-8095(01)00133-8, 2002.

Finke, U. and Hauf, T.: The characteristics of lightning occurrence in southern Germany, Contr. Atmos. Phys., 69, 361–374, 1996.

Heiblum, R. H., Koren, I., and Altaratz, O.: Analyzing coastal precipitation using TRMM observations, Atmos. Chem. Phys., 11, 13201–13217, doi:10.5194/acp-11-13201-2011, 2011.

Hojo, J., Ishii, M., Kawamura, T., Suzuki, F., Komuro, H., and Shiogama, M.: Seasonal variation of cloud-to-ground lightning flash characteristics in the coastal area of the Sea of Japan, J. Geophys. Res., 941, 13207–13212, doi:10.1029/JD094iD11p13207, 1989.

Kahana, R., Ziv, B., Enzel, Y., and Dayan, U.: Synoptic climatology of major floods in the Negev Desert, Israel, Int. J. Climatol., 22, 867–822, doi:10.1002/joc.766, 2002.

Kanamitsu, M.: Description of the NMC global data assimilation and forecast system, Weather Forecast., 4, 335–342, doi:10.1175/1520-0434(1989)004<0335:DOTNGD>2.0.CO;2, 1989.

Katz, E. and Kalman, G.: The impact of environmental and geographical conditions on lightning parameters derived from lightning location system in Israel, in: Proceeding of the 10th International Symposium on Lightning Protection, Curitiba, Brazil, November, 9–13 November 2009, 249–254, 2009.

Kitagawa, N. and Michimoto, K.: Meteorological and electrical aspects of winter thunderclouds, J. Geophys. Res., 99, 10713–10721, doi:10.1029/94JD00288, 1994.

Levin, Z., Yair, Y., and Ziv, B.: Positive cloud-to-ground flashes and wind shear in Tel-Aviv thunderstorms, Geophys. Res. Lett., 23, 2231–2234, 1996.

Mackerras, D. and Dmweniza, M.: Latitudinal variation of lightning occurrence characteristics, J. Geophys. Res., 99, 10813–10821, doi:10.1029/94JD00018, 1994.

Manoochehrnia, P., Rachidi, F., Rubinstein, M., and Schulz, W.: Lightning Statistics in Switzerland, in: Proceedings of the International Symposium on Lightning Protection, Foz Do Iguassu, Brazil, 26–30 November 2007, 2007.

Lightning characteristics in Eastern Mediterranean thunderstorms

Y. Ben Ami et al.

Title Page

Abstract	Introduction
Conclusions	References
Tables	Figures

◄◄   ►►

◄   ►

Back   Close

Full Screen / Esc

Printer-friendly Version

Interactive Discussion

Matsui, M. and Hara, Y.: The characteristics of winter lightning in Hokkaido as observed by the JLDN, Lightning Protection (ICLP), 2014 International Conference, Shanghai, China, 11–18 October, 116–121, 2014.

Orville, R. E, Weisman, R. A., Pyle, R. B., Henderson, R. W., and Orville Jr., R. E.: Cloud-to-ground lightning flash characteristics from June 1984 through May 1985, J. Geophys. Res., 92, 5640–5644, doi:10.1029/JD092iD05p05640, 1987.

Pierce, E. T.: Latitudinal variation of lightning parameters, J. Appl. Meteorol., 9, 194–195, doi:10.1175/1520-0450(1970)009<0194:LVOLP>2.0.CO;2, 1970.

Prentice, S. A. and Mackerras, D.: The ratio of cloud to cloud-ground lightning flashes in thunderstorms, J. Appl. Meteorol., 16, 545–550, doi:10.1175/1520-0450(1977)016<0545:TROCTC>2.0.CO;2, 1977.

Rakov, V. A. and Uman, M. A.: Lightning: Physics and Effects, Cambridge Univ. Press, Cambridge, UK, 687 pp., 2003.

Randell, S. C., Rutledge, S. A., Farley, R. D., and Helsdon Jr., J. H.: A modeling study on the early electrical development of tropical convection: continental and oceanic (monsoon) storms, Mon. Weather Rev., 122, 1852–1877, doi:10.1175/1520-0493(1994)122<1852:AMSOTE>2.0.CO;2, 1994.

Saunders, C. P. R.: Charge generation and separation charge separation mechanisms in clouds, Saunders, Space Sci. Rev., 137, 335, doi:10.1007/s11214-008-9345-0, 2008.

Saunders, C. P. R., Keith, W. D., and Mitzeva, R. P.: The effect of liquid water on thunderstorm charging, J. Geophys. Res., 96, 11007–11017, doi:10.1029/91JD00970, 1991.

Shalev, S., Saaroni, H., Izsak, T., Yair, Y., and Ziv, B.: The spatio-temporal distribution of lightning over Israel and the neighboring area and its relation to regional synoptic systems, Nat. Hazards Earth Syst. Sci., 11, 2125–2135, doi:10.5194/nhess-11-2125-2011, 2011.

Shay-El, Y. and Alpert, P.: A diagnostic study of winter diabatic heating in the Mediterranean in relation to cyclones, Q. J. Roy. Meteor. Soc., 117, 715–747, doi:10.1002/qj.49711750004, 1991.

Suzuki, T.: Long term observation of winter lightning on Japan Sea Coast, Res. Lett. Atmos. Electr., 12, 53–56, 1992.

Suzuki, T., Matsudo, Y., Asano, T., Hayakawa, M., Michimoto, K.: Meteorological and electrical aspects of several winter thunderstorms with sprites in the Hokuriku area of Japan, J. Geophys. Res., 116, D06205, doi:10.1029/2009JD013358, 2011.

Lightning characteristics in Eastern Mediterranean thunderstorms

Y. Ben Ami et al.

Title Page

Abstract	Introduction
Conclusions	References
Tables	Figures

◄◄   ►►

◄   ►

Back   Close

Full Screen / Esc

Printer-friendly Version

Interactive Discussion

Takahashi, T.: Riming electrification as a charge generation mechanism in thunderstorms, J. Atmos. Sci., 35, 1536–1548, doi:10.1175/1520-0469(1978)035<1536:REAACG>2.0.CO;2, 1978.

Williams, E. and Renno, N.: An analysis of the conditional instability of the Tropical Atmosphere, Mon. Weather Rev., 121, 21–36, doi:10.1175/1520-0493(1993)121<0021:AAOTCI>2.0.CO;2, 1993.

Williams, E. and Stanfill, S.: The physical origin of the land-ocean contrast in lightning activity, C. R. Phys., 3, 1277–1292, doi:10.1016/S1631-0705(02)01407-X, 2002.

Williams, E., Mushtak, V., Rosenfeld, D., Goodman, S., and Boccippio, D.: Thermodynamic conditions favorable to superlative thunderstorm updraft, mixed phase microphysics and lightning flash rate, Atmos. Res., 76, 288–306, doi:10.1016/j.atmosres.2004.11.009, 2005.

Williams, E. R. and Yair, Y.: The microphysical and electrical properties of sprite producing thunderclouds, in: Sprites, Elves and Intense Lightning Discharges, edited by: Fullekrug, M. et al., Springer, Dordrecht, the Netherlands, 57–83, 2006.

Yair, Y., Levin, Z., and Altaratz, O.: Lightning phenomenology in the Tel-Aviv area from 1989 to 1996, J. Geophys. Res., 103, 9015–9025, doi:10.1029/98JD00087, 1998.

Yair, Y., Shalev, S., Erlich, Z., Agrachov, A., Katz, E., Saaroni, H., Price, C., and Ziv, B.: Lightning flash multiplicity in eastern Mediterranean thunderstorms, Nat. Hazards Earth Syst. Sci., 14, 165–173, doi:10.5194/nhess-14-165-2014, 2014.

Ziv, B. and Yair, Y.: The weather in Israel, Unit 5, Hebrew, in: Introduction to Meteorology, The Open University Press, Tel Aviv, Israel, 5–59, 1994.

Ziv, B., Saaroni, H., Ganot, M., Yair, Y., Baharad, A., and Isaschari, D.: Atmospheric factors governing winter lightning activity in the region of Tel Aviv, Israel, Theor. Appl. Climatol., 95, 301–310, doi:10.1007/s00704-008-0008-6, 2009.

Title Page

Abstract | Introduction

Conclusions | References

Tables | Figures

|◄ | ►|

◄ | ►

Back | Close

Full Screen / Esc

Printer-friendly Version

Interactive Discussion

Table 1. Criteria used for classification of synoptic systems.

Synoptic	Location of center of low system pressure at sea level		Wind direction at 925 hPa	
	North or west of the Israeli coast	South or southeast of Israel	Northwest to southwest	Northeast to southeast
WCL and FCL	✓	✗	✗	✓
RST-CL	✓	✓	✓	✗
RST	✗	✓	✗	✓

Figure 1. Distribution of peak currents during WCL system [25 km^2]. Data is plotted as a function of longitudes (**a** and **c**) and latitudes (**b** and **d**). Distributions are calculated for steps of 5 kA in peak current intensities. (**a** and **b**) are for peak currents between 0 and -25 kA and (**c** and **d**) present the range between -25 and -45 kA. Black boxes mark a distance of 250 km from the center of the ILLS which is marked by black arrows. Absolute currents larger than 45 kA are not shown.
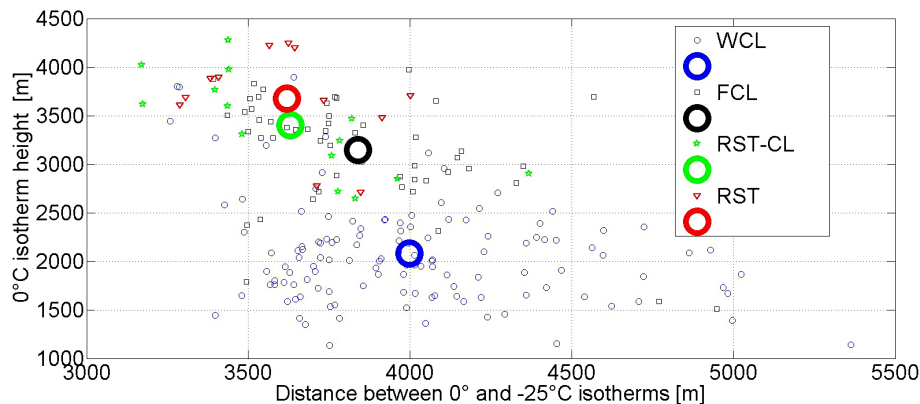
Figure 2. The 0 °C isotherm height above sea level as a function of the depth (thickness) of the atmospheric layer between 0 and −25 °C [m]. Results are based on geopotential height of the 0 and −25 °C isotherms using the GDAS database for the area between 32–33° N and 34–35° E. Centroids for the four subsets are marked with circles.
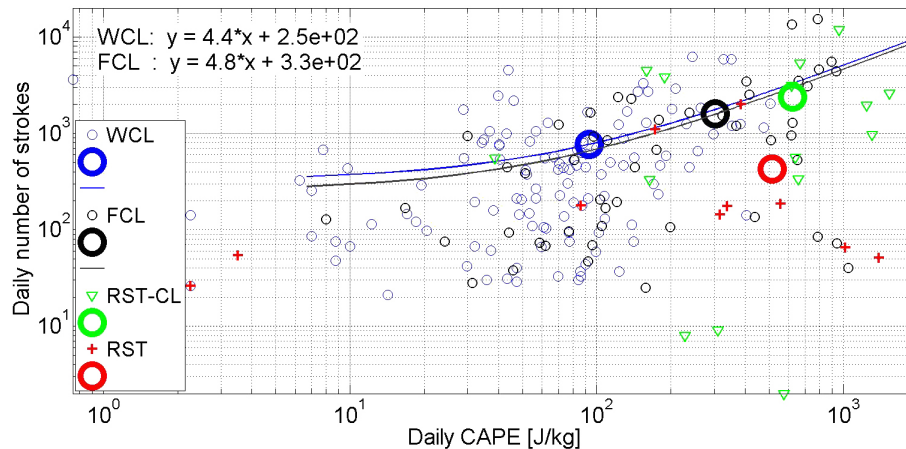
Figure 3. Number of strokes per day as a function of CAPE according to the four synoptic systems. The CAPE is taken from the GDAS dataset for the area between 32–33° N and 34–35° E. Centroids for the four subsets are marked by circles and linear fit for WCL and FCL are shown in blue and black curves respectively.
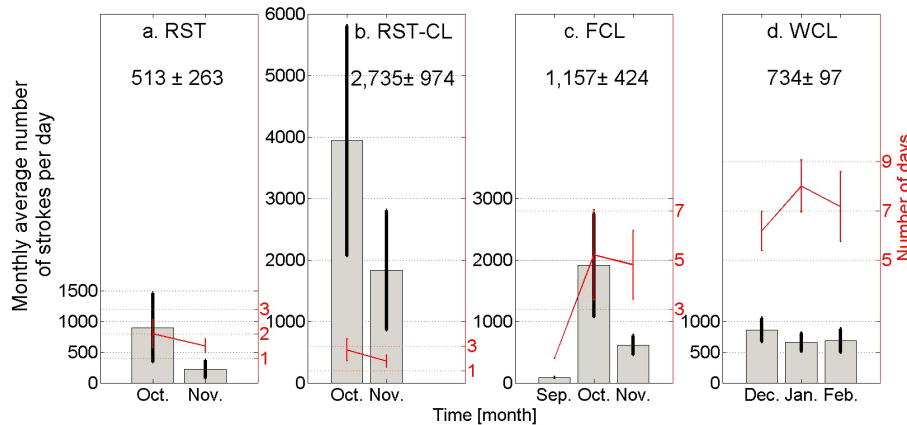
Figure 4. Inter-annual monthly average number of strokes per day (bar) and the average number of days (red curve) for the four synoptic systems. The error-bars indicate standard errors. Seasonal perennial-monthly mean and standard error are shown for each system.

Full Screen / Esc

Figure 5. Strokes density per $25\,km^2\,day^{-1}$ according to the four synoptic systems. To highlight spatial features and to compare between all systems a similar color-bar is used. Maximum values per $25\,km^{-2}\,day^{-1}$ are 37 in WCL, 54 in FCL, 33 in RST and 131 in RST-CL. Red circles mark a distance of $250\,km$ from the approximated center of the ILLS which is located in the center of Israel.
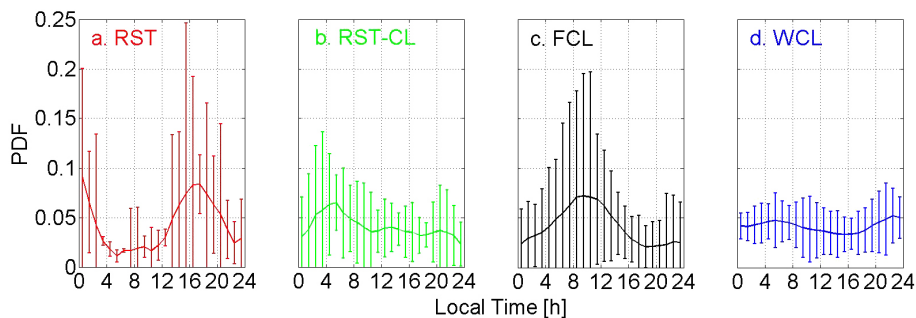
Figure 6. Diurnal PDF of lightning strokes in local time according to the four synoptic systems. The integral under each curve equals one. Error-bars indicate inter-annual STD.
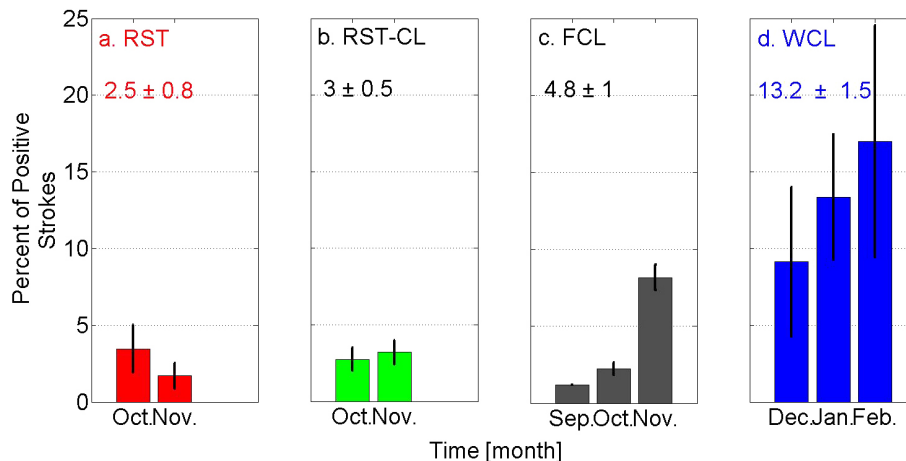
Figure 7. Inter-annual monthly mean fraction of positive strokes according to the four synoptic systems. The error-bars indicate the perennial-monthly standard error. Seasonal perennial-monthly mean and standard error are shown for each system.

NHESSD

3, 3655–3685, 2015

Lightning characteristics in Eastern Mediterranean thunderstorms

Y. Ben Ami et al.

Title Page

Abstract | Introduction

Conclusions | References

Tables | Figures

|◄ | ►|

◄ | ►

Back | Close

Full Screen / Esc

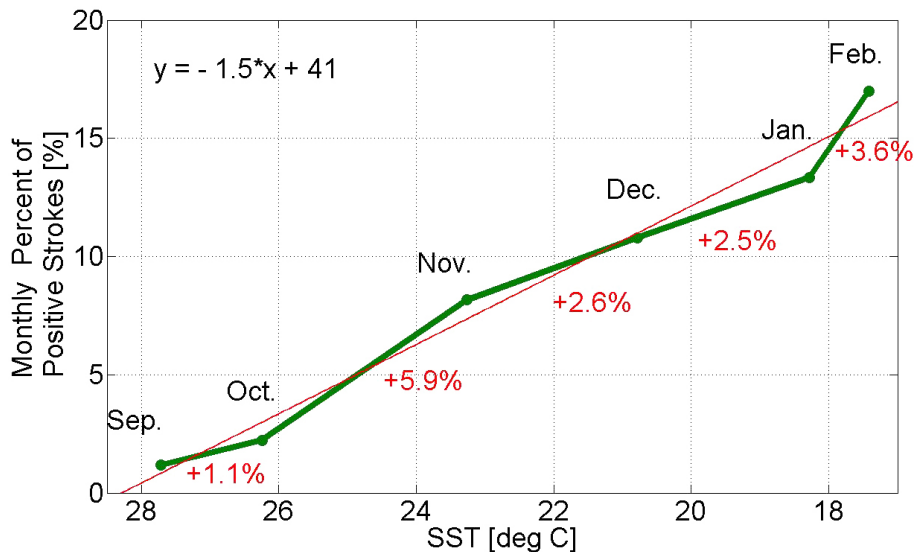Printer-friendly Version

Interactive Discussion

Figure 8. Monthly mean fraction of positive strokes for FCL and WCL systems, between September and February, as a function of the monthly mean SST (green). Note the reverse *x* axis. Linear fit between the two variables is plotted in red and the average increases per month are marked by red numbers near the curve. SST is calculated based on retrieval from MODIS Aqua, using the 11 μm band for the area between 32–36° E and 30–34° N.
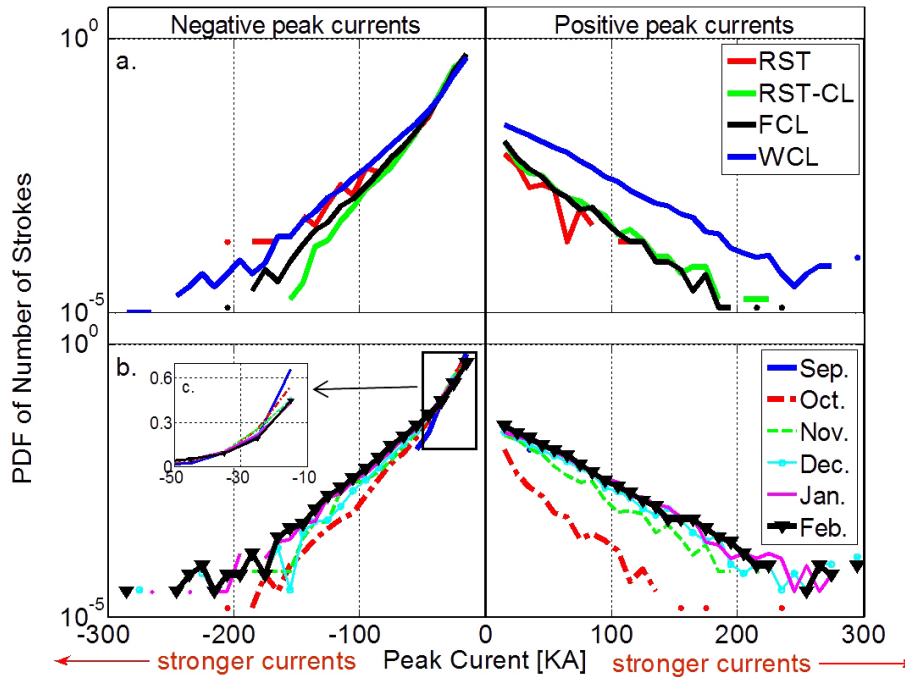
Figure 9. (a) PDF of peak currents [kA] in logarithmic scale as a function of synoptic system. The integral under each curve of positive and negative strokes per synoptic system equals one; **(b)** monthly PDF for systems of FCL and WCL only in logarithmic scale; **(c)** zoom-in window for the area between −35 and −10 kA, marked with black box on panel **(b)**: it highlights the temporal decrease in fraction of negative weak currents.